PII: S0032-3861(96)00638-6

Polymer Vol. 38 No. 6, pp. 1345–1356, 1997

0032-3861/97/$17.00 + 0.00

Chemical modification of a Nafion® sulfonyl fluoride precursor via *in situ* sol–gel reactions

A. J. Greso, R. B. Moore, K. M. Cable, W. L. Jarrett and K. A. Mauritz*
Department of Polymer Science, University of Southern Mississippi, Southern Station Box 10076, Hattiesburg, MS 39406-0076, USA
(Received 28 October 1995; revised 3 June 1996)

The melt-processible sulfonyl fluoride precursor of a Nafion® ionomer was utilized as a sol–gel reaction medium for 3-aminopropyltriethoxysilane (APrTEOS). The diffusion-mediated reaction of APrTEOS with SO_2F groups can be controlled with high degree of reaction. Fourier transform infra-red/attenuated total reflection studies show that sulfonamide linkages are formed and condensation reactions of SiOR groups provide covalent crosslinking of chains. Formic acid treatment plus high temperature plus long time resulted in a high degree of polymer crosslinking as seen in ^{29}Si solid state nuclear magnetic resonance spectra. Mechanical modulus and strength increase, and elongation-to-break decreases with increasing filler. Hybrids with <18% uptake accumulate cracks with crosslinked outer layers, each event signalled by a drop in stress followed by stress recovery. While there are sharp visual material fronts inward from both surfaces, EDAX (energy dispersive analysis of X-rays) showed that there are no sharp Si composition boundaries. Differential scanning calorimetry (d.s.c.) revealed a broad, weak endothermic event peaking at 67°C for the precursor and shifting to higher temperatures while broadening with increasing filler content, indicating progressively-restrictive glass-transition-temperature-related molecular motions within an increasingly nonhomogeneous environment. For the unreacted precursor, this d.s.c. transition occurs at a temperature just above a glass transition detected by dynamic mechanical means.

(Keywords: Nafion®; sulfonyl fluoride precursor; *in situ* sol–gel chemistry; crosslinking)

INTRODUCTION

This work is a component of our broader program to formulate perfluoro-organic/[inorganic oxide] hybrid materials via sol–gel reactions for inorganic alkoxides and organoalkoxysilanes in Nafion® films[1–6]. Nafion® is a successful membrane material used in large scale chlorine and caustic production via electrochemical cells and is a strong contender as a fast proton-conducting separator in fuel cells for electrical power generation.

In this work, we utilize a melt-processible sulfonyl fluoride precursor of a Nafion® ionomer as the sol–gel reaction medium for 3-aminopropyltriethoxysilane (APrTEOS). The chemical structure of this ionomeric precursor is:

$$[CF_2CF(CF_2CF_2)_n]_m$$
$$\backslash$$
$$OCF_2CFCF_3$$
$$\backslash$$
$$OCF_2CF_2SO_2F$$

The proposed reaction between APrTEOS and SO_2F groups at the ends of the sidechains is: $-SO_2F + (EtO)_3-Si-Pr-NH_2 \rightarrow (EtO)_3-Si-Pr-NHSO_2- + HF$. Given sufficient mobility and proximity of $-Si(OEt)_3$ endgroups on different sidechains, subsequent H_2O addition will initiate condensation reactions that crosslink the polymer chains via Si–O–Si bridges and create a covalently-bound inorganic phase. In future experiments, unreacted SiOR groups could serve as sites with which subsequently-diffusing $(RO)_{4-x}Si(OH)_x$ molecules, for example, can react forming additional Si–O–Si bridges and, after drying, yield silicon oxide particles that are chemically bound to the matrix.

The approach is based in part upon prior work, using simpler molecules, done by Covitch *et al.*[7], Hsu[8], and Grot[9], who showed that primary amines can permeate Nafion® precursor films and react with SO_2F groups to change the swelling and mechanical properties of this polymer.

Owing to the resistance of these hydrophobic precursor films to swelling in the polar solvents for silicon alkoxides, the incorporation of silicon oxide phases via sol–gel chemistry has not been attempted. However, the melt-processibility of the precursor polymer, which exhibits crystallite melting around 265°C[10], can be viewed as a useful parameter in affecting physical modifications of these materials, say by a combination of mechanical orientation and thermal processes. The $-SO_2F$ form stands in contrast with the hydrolysed forms which are non-melt-processible and insoluble under ordinary conditions owing to ionic crosslinking.

In the work that follows, degree of reaction vs time was followed gravimetrically. Fourier transform infra-red (*FT* i.r.) and ^{29}Si solid state nuclear magnetic resonance

* To whom correspondence should be addressed

(n.m.r.) analyses of the molecular structures of the incorporated phases, and their coupling to the side-chains, were conducted for different reaction conditions. Tensile stress–strain profiles and mechanical failure mechanisms were explored in conjunction with optical/electron microscopic investigations of surface and cross sectional morphologies. Cross sectional morphologies were compared against Si composition profiles along the membrane thickness direction. Thermal transitions and thermal degradation were investigated using differential scanning calorimetry (d.s.c.), dynamic mechanical analysis (d.m.a.) and thermogravimetric analysis (t.g.a.) techniques.

EXPERIMENTAL

Materials and sample preparation

As-received sulfonyl fluoride precursor films, obtained from E.I. DuPont Co., had, in the ionized form, an equivalent weight of approximately 1100 and nominal thickness of 0.007 in (0.178 mm). The particular sheet from which samples were cut actually had a thickness that varied from about 0.165 mm near the edges to 0.210 mm in the centre.

APrTEOS, obtained from Aldrich Co., was used as-received. Pure ethanol was used to leach excess unreacted APrTEOS from treated samples. Prior to reacting with APrTEOS, samples were soaked in the solvent perfluorohydrophenanthrene, known commercially as Flutec®. Unless otherwise indicated, samples were soaked in Flutec® for 48 h at 23°C, then dried for 27 h under vacuum at 102°C. Flutec®, having a boiling point of 215°C, is capable of dissolving the Nafion® precursor at high temperatures and can cause considerable swelling at room temperature. The latter fact is of critical importance in these experiments. For example, the percent weight gain of as-received samples due to swelling in this solvent for 2 days at room temperature can be somewhat above 200%. If as-received samples are annealed, the uptakes are lower, which may be related to increased crystallinity. It is seen in all cases that, upon drying, the weight is lower than the dry, pre-swollen weight, indicating that a soluble fraction of the polymer has been leached out by invasive Flutec®. In a few cases, where indicated, formic acid was used for accelerating the sol–gel reaction of APrTEOS.

Circular-shaped sulfonyl fluoride form samples of diameter 2.54 cm were placed directly into 20 ml, APrTEOS-filled borosilicate scintillation vials, at 23°C, that were sealed with polyurethane caps. In the reaction between APrTEOS and $-SO_2F$ groups, HF released in this reaction might be considered to react with the glass vial; if so, the byproducts are assumed to not influence the reaction within the polymer. Polymer samples were left in the vials for the prescribed times noted in Results and Discussion. The samples were then placed in scintillation vials containing EtOH and left for 24 h; this step was repeated so as to remove excess unreacted APrTEOS. After the second ethanol soak, the wet samples were sandwiched between the bottoms of two petri dishes. This arrangement kept the films flat while the samples were in an oven at 102°C under full vacuum. The samples were left in the oven for 24 h except where noted otherwise. The samples were weighed prior to soaking in APrTEOS and after drying in the vacuum oven.

In order to understand the more complex polymer-*in-situ* reactions, APrTEOS was reacted with itself in the bulk liquid state. APrTEOS was initially exposed to air at 50% relative humidity and 24°C for 4 and 24 h in petri dishes with no solvent. In this condition, hydrolysis and condensation reactions are possible. The resultant products were analysed using ^{29}Si solid state n.m.r. spectroscopy and t.g.a.

Instrumentation and methods

Weight changes. Gravimetric determinations of samples before and after the various preparative steps were made with a Mettler AJ100 piezoelectric balance calibrated to ±0.0001 g and consistently within ±0.0002 reproducible error.

N.m.r. and FT*i.r. spectroscopy.* Solid state n.m.r. spectra were acquired using a Bruker MSL-400 NMR spectrometer operating at a frequency of 79.5 MHz for ^{29}Si. A standard double air bearing CP/MAS probe was used. Samples were loaded into 4 mm fused zirconia rotors and sealed with Kel-F™ caps. Spectra were obtained using magic angle spinning with high power decoupling during acquisition only and a spinning rate of 3600 Hz. A modified version of the DEPTH sequence[11] was used to suppress ^{29}Si background due to the probe. The 90° pulse width was 5.0 μs, the probe dead time was 13 μs and the acquisition time was 45 ms. The recycle delay was 180 s. All chemical shifts were referenced externally to the downfield peak of tetrakis(trimethylsilyl)silane (−9.8 with respect to TMS). The independently-reacted APrTEOS bulk sample, in the process of gelation, was run for lengths of time noted in Results and Discussion. The composite films were cut into small fragments and around 0.2 g of these were packed into the tube.

FT i.r. spectra of samples were obtained with a Bruker IFS88, operating with a Spectra Physics attenuated total reflection (ATR) attachment using a thallium bromide-iodide crystal (KRS-5) oriented at 45° and employing 100 counts at 22°C. Parts of individual samples were

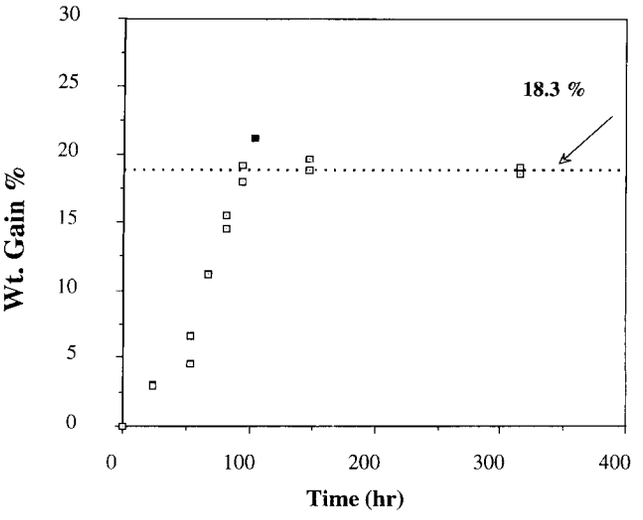

Figure 1 Percent weight gain of Nafion® SO_2F precursor vs time of exposure to APrTEOS. After exposure to APrTEOS, samples were soaked in EtOH, then heated at 102°C *in vacuo*. The deviant point at 21.5%, 103 h, was generated by exposing the sample to atmospheric moisture between the two soakings in EtOH

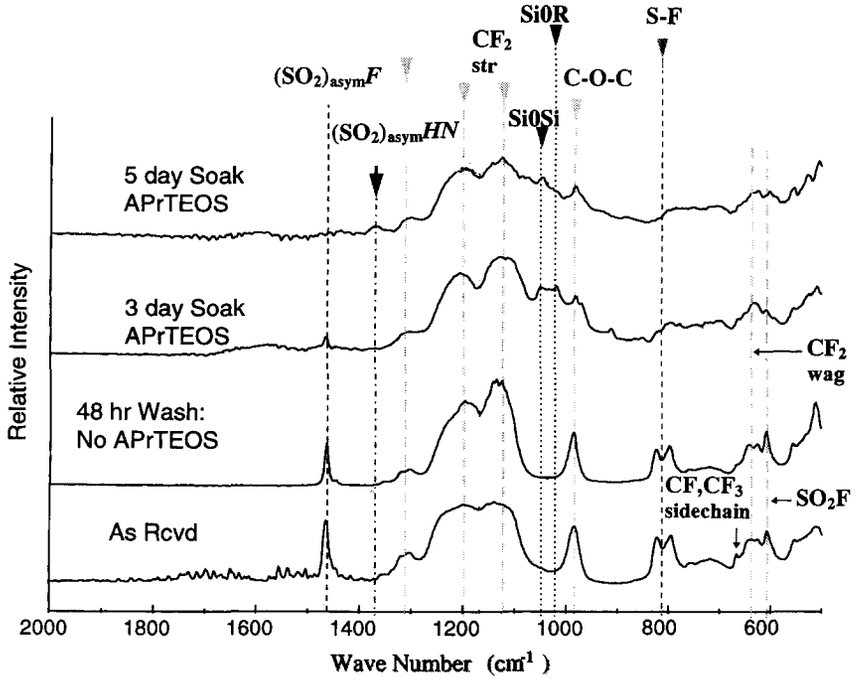

Figure 2 *FT*i.r./ATR spectra of Nafion®-SO_2F: (a) as-received, (b) Flutec®-washed, but unreacted and (c), (d) APrTEOS-reacted for 3 and 5 days, respectively, as indicated

mounted along both sides of the crystal. A Flutec® spectrum was acquired in transmission mode through NaCl windows.

Microscopy and silicon oxide concentration profiles. Optical micrographs, using transmitted light, were obtained using a Nikon OPTIPHOT-POL microscope and camera. An Electroscan E-20 environmental scanning electron microscope (ESEM) fitted with a Tracor Northern interfaced Noran System II backscatter X-ray detector (EDAX) was used to determine the elemental peak intensity ratio Si/S. As in our earlier studies[3,6], the intensity of the sulfur peak was considered as an internal reference as the intensities of incorporated elements are normalized in relation to the number of SO_2 groups in the sidechains. This ratio was determined spot-by-spot across film thicknesses for samples reacted for various times in APrTEOS. The polymer samples were held in liquid N_2 prior to freeze-fracturing in order to generate fresh cross sections for ESEM viewing.

Mechanical analyses. Mechanical stress vs strain profiles were obtained using an Instron tensile testing machine with a special gear ratio converter. All samples were elongated at the crosshead speed 0.78 mm min^{-1} using an interfaced computer. Tests were performed on samples that were die-punched from films into a dogbone shape. These samples were placed between small rubber-mounted grips and pulled with a 5.00 kg load cell. The gauge length and width of the dogbones were 10 and 3 mm respectively.

The tensile runs of as-received, untreated, precursor samples were truncated after 400% extension as these films had a tendency to pull out of the grips after extended periods of time before failure. On the other hand, all APrTEOS-treated samples failed prior to 50% strain with no discernible pullout from the grips.

Nafion® precursor samples were dried at only 102°C after soaking in Flutec®, as it was noted that samples that were dried at 120°C were in a warped state after soaking, and remained warped after reacting with APrTEOS. At present, we cannot account for this phenomenon in terms of temperature-induced structural changes under the influence of this solvent. The condition of warped, brittle samples encouraged premature failure during placement in grips whether or not the samples were treated with formic acid. Lesser but notable difficulties were encountered with films evacuated at the lower temperature of 110°C.

The results presented are for samples for which fracture occurred in the middle rather than at the grips. The results for samples that fail in this way were seen to be reproducible.

Dynamic mechanical measurements were performed on sulfonyl fluoride precursor films using a Seiko Instruments SDM 5600 Series dynamic mechanical spectrometer (DMS 200). Samples were analysed in the tensile mode from −100°C to 125°C at 1 Hz.

Differential scanning calorimetry and thermogravimetric analysis. D.s.c. and t.g.a. analyses were performed using a Mettler DSC 30 and a Mettler TG50, respectively. Each were operated with heating and cooling rates of 10°C min^{-1} under N_2. Temperature programs for all d.s.c. runs consisted of heating the material up to 230°C and cooling back to 30°C—twice in succession—with one minute pauses at 30 or 230°C prior to re-heating or re-cooling. These limits were established after running the TG50 independently, with either the polymer-based materials or singly-reacted APrTEOS from 50°C up to 280°C. The mass of each d.s.c. sample was 7 ± 0.5 mg; masses for the t.g.a. samples were 20 ± 0.5 mg.

RESULTS AND DISCUSSION

Uptake of APrTEOS-reacted samples vs time

Film thickness variation was responsible for variation of untreated sample weight, from about 0.1850 g to 0.2150 g, for the fixed 2.54 cm diameter of the disks.

Figure 1 shows weight gain as a function of time of film exposure to liquid APrTEOS at room temperature (23°C). As mentioned, after exposure to this agent for the indicated times, the samples were removed from the liquid and excess, unbonded reactants leached out in two steps in EtOH after which the samples were heated at 102°C under vacuum. The percent uptake reaches an asymptotic level of 18.3% within 96 h (4 days). This asymptotic uptake might be converted to an average degree of reaction involving a combination of a degree of sulfonamide formation and a degree of hydrolysis–condensation reaction of $Si(OEt)_3$ groups, given the equivalent weight of the polymer and molecular weight of APrTEOS. However, it will be seen that such a crude calculation is meaningless as the distribution of reaction products is very non-uniform across the film thickness. This weight percent is not realized if the samples are not vacuum-dried prior to weighing. In this situation, the samples become cloudy as a consequence of hydrolysis-condensation reactions initiated by atmospheric moisture. The deviant data point in *Figure 1*, showing 21.5% gain at 103 h, was generated by exposing the sample to air for a long time between the two soakings in EtOH. This is the single example on this curve of a cloudy sample prepared in this undesirable way.

If the samples were not soaked in Flutec®, followed by their drying, they were only capable of achieving 15.5% uptake. Thus, pre-soaking in the perfluorinated solvent increases the permeability of the precursor for APrTEOS. We also note another important fact: After soaking in Flutec® and drying, the polymer suffers a weight loss of around 3%. The observance of the increase in APrTEOS reaction capacity from 15.5 to 18.3%, combined with the Flutec®-induced weight loss, suggests that low molecular weight polymer fragments that are inert to amine reaction, are leached out of the films.

FT*i.r./ATR spectroscopy*

I.r. spectra, displayed in *Figure 2*, show definite chemical transformations resulting from the sample preparative steps. These spectra do not have the same vertical absorbance scale, so that they can be compared more easily. While the bands of direct relevance to the chemical modifications affected in this work are noted in this figure, the remaining peaks have been noted in earlier reports[7,8,12,13].

The sharp peak $\sim 1470\,cm^{-1}$ seen for the as-received sulfonyl fluoride precursor (bottom spectrum) is attributed to asymmetric $-SO_2-$ stretching in the SO_2F group. The twin peaks $\sim 810\,cm^{-1}$ are due to S–F stretching vibrations of the SO_2F group. Diminishment or disappearance of the $\sim 1470\,cm^{-1}$ peak, as well as of the twin peaks $\sim 810\,cm^{-1}$, reflects chemical conversions of the SO_2F group. Both the as-received sample as well as solvent-soaked sample (spectrum second from bottom) retain the characteristic SO_2F absorbances in these two regions. After exposure of the Flutec®-soaked samples to APrTEOS for 3 days, followed by EtOH leaching, then drying, the absorbance in the $\sim 810\,cm^{-1}$ region essentially disappears while the $\sim 1470\,cm^{-1}$ band becomes very weak. After APrTEOS permeation plus reaction for 5 days, both bands in fact disappear. Thus, we conclude that most SO_2F groups have undergone chemical conversion.

The conversion of sulfonylhalide groups to sulfonamide groups is signalled by considerable shifting of the asymmetric $-SO_2-$ stretching peak ($\sim 1470\,cm^{-1}$ in this case, for the former) to lower wavenumbers[14,15]. A weak peak in the region of asymmetric stretching in $-SO_2-$ groups in these linkages $\sim 1375\,cm^{-1}$ does in fact appear for the sample that was treated for 5 days, although not for the 3 day-treated sample. We are not aware of whether this absorption is intrinsically weak, but a low degree of reaction clearly does not exist because of the disappearance of the two SO_2F-related absorbances. Moreover, the intrinsically strong $-NH_2$ bending vibration[16] is not seen in its characteristically broad region around $1600\,cm^{-1}$ in the upper two spectra.

Hsu[17] discusses a temperature-sensitive doublet between 600 and $700\,cm^{-1}$ associated with CF_2 wagging as being the signature of helix reversal along the Nafion® backbone. This feature is evident $\sim 640\,cm^{-1}$ in the bottom two spectra in *Figure 2*, although the peaks appear to merge upon APrTEOS treatment. Hsu also discusses a peak at $606\,cm^{-1}$ which appears in the spectrum of the SO_2F form but not in the spectrum of PTFE. This peak is also seen distinctly in *Figure 2*. Hsu observed that this peak was reduced to insignificance upon treatment with ethylene diamine which produced sulfonamide groups, leading him to conclude that the band was associated with the SO_2F moiety. In our spectra, this peak is rather diminished but not entirely absent upon treatment with APrTEOS. Finally, Hsu notes the presence of a shoulder at $655\,cm^{-1}$ assigned to CF or CF_3 groups in sidechains. A weak peak in this position, which diminishes upon solvent soaking, was also seen in our spectra.

The peak $\sim 980\,cm^{-1}$ is due to symmetric stretching within C–O–C groups in the side chains[18]. This prominent absorbance becomes obscured with APrTEOS treatment which introduces bands characteristic of silicon oxide compounds.

Seen in the upper two spectra is a decrease, upon increasing time of sample exposure to APrTEOS, in the absorbance associated with the Si–O–Et groups relative to the absorbance attributed to asymmetric stretching within Si–O–Si groups. Thus, we conclude that condensation reactions between APrTEOS groups has occurred. The consequence of this as well as other evidence is that interchain crosslinking is present. While the 102°C vacuum/heat treatment may be insufficient to ensure maximum condensation among available SiOR sites, these results suffice to demonstrate that this reaction can occur *in situ*.

A very strong bimodal absorption envelope with maxima ~ 1200 and $\sim 1150\,cm^{-1}$ in the region of CF_2 stretching[18] is seen for all samples. The fact that these peaks, which are very broad for the as-received sample, become sharper after this sample was soaked in Flutec®, then dried, might be additional evidence that soluble CF_2-containing fragments are extracted from the polymer. On the other hand, the $810\,cm^{-1}$ doublet does not change significantly and the 980 cm^{-1} and $1470\,cm^{-1}$ peaks, all three features being sidechain fingerprints, become somewhat narrower.

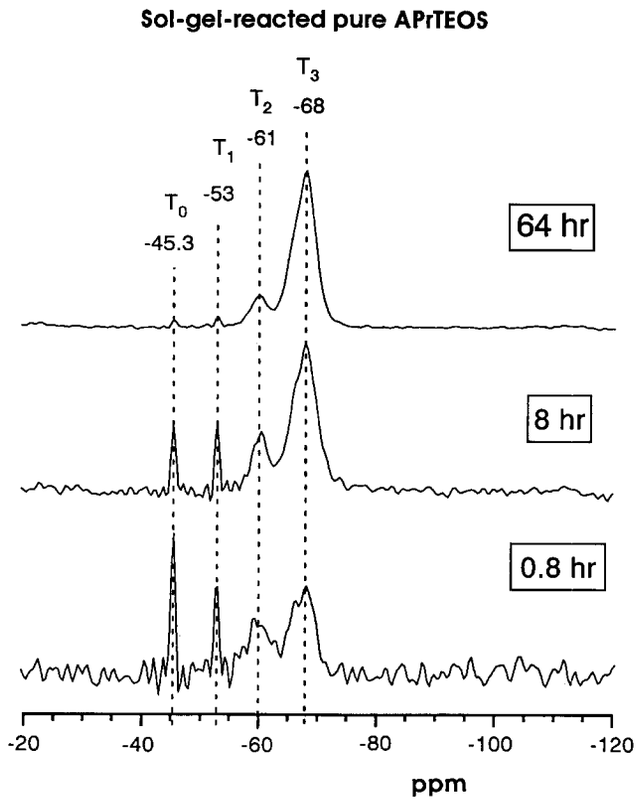

Figure 3 ^{29}Si solid state n.m.r. spectra of APrTEOS undergoing bulk sol–gel reactions vs reaction time, or varying number of scans. Bottom spectrum was acquired after 48 min (16 scans), the middle spectrum after 8 h (160 scans), and top spectrum after 64 h (1280 scans). T_n peaks are indicated

Presently unaccounted for is a peak $\sim$1300 cm^{-1} in all four spectra. We have noted that the spectrum of pure Flutec® contains a strong, broad absorbance band in this wavenumber region and has the same shape as the same bimodal shape as the peak in *Figure 2*. This fact would have relevance if the as-received membrane contained residual Flutec® as a result of its processing.

^{29}*Si solid state n.m.r. spectroscopy*

Figure 3 shows time-dependent spectra taken during the gelation of pure APrTEOS within the rotor of the solid state n.m.r. spectrometer using high powered decoupling with a recycle time of 180 s. The fact that the sample containers were capped might influence the reaction with regard to vapour pressure build-up therein. Shown in *Figure 3* are the time-averaged, or *cumulative* results of spectra taken over the indicated times. While this procedure results in lower noise/signal, spectra taken during longer times retain signal information present during initial gelation. Thus, for example, the 64 h spectrum contains an accumulation of peak information gathered up to that time.

The four peaks, ranging from −45.3 to −68 ppm, are labelled as T_0, T_1, T_2, and T_3, in order. These peaks are associated with $n = 0$, 1, 2 and 3, respectively, in the grouping—Pr–**Si**$(OR)_{3-n}$(O–Si–Pr–)$_n$. The low-order T_n peaks are not prominent in the cumulative spectrum for 64 h owing to the advanced degree of SiOR group condensation. *Figure 3* was obtained for the simple purpose of identification of the peaks corresponding to the different states of Si atom coordination about

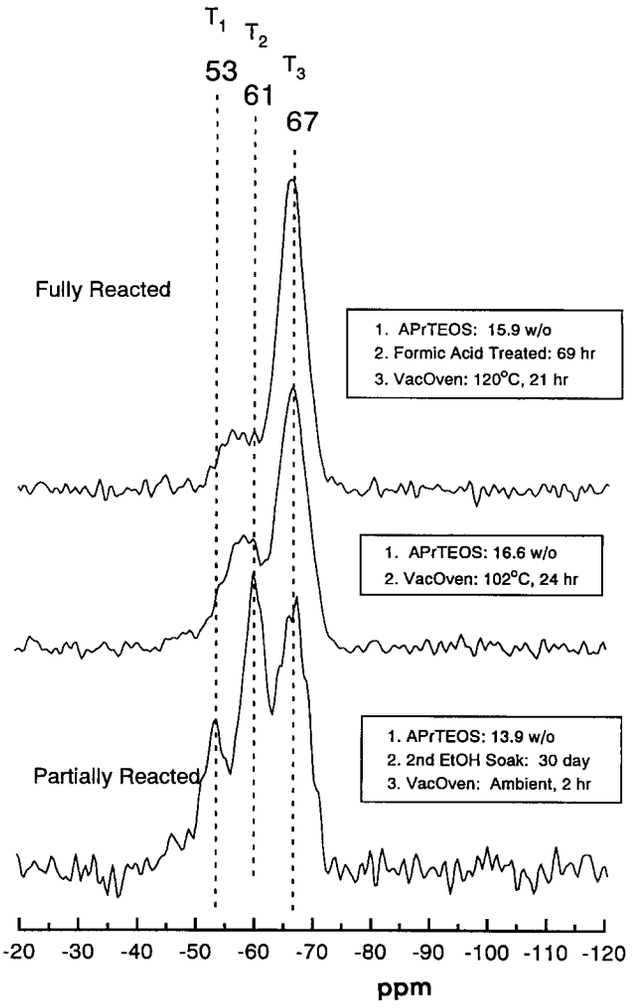

Figure 4 ^{29}Si solid state n.m.r. spectra of composites of indicated compositions and preparation conditions. Excess APrTEOS was removed prior to examination

$CSiO_3\equiv$ groups that have evolved during the course of the sol–gel reaction.

The 0.8 h sol–gel-reacted spectrum, while having a low signal-to-noise ratio, shows clear peaks at −45.3, −53, −59 and −68 ppm. The −45.3 ppm peak exactly corresponds to the literature assignment of unreacted APrTEOS[19], i.e. T_0, where Si is attached to one propyl and three ethoxy groups. The chemical shift reported for $(SiO)_3SiCH_3$, i.e. T_3, is −65 ppm[20] which is somewhat close to −68 ppm. As time continues, the initially-prominent T_0 peak intensity drops below those of the other peaks as the chemical shift distribution moves rightward, indicating an increase in the average number of –Pr–Si–O–Si–Pr- bonds forming between APrTEOS molecules. The 63-h spectrum indicates that most of the ethoxy groups of APrTEOS molecules have undergone hydrolysis and condensation reactions thereby crosslinking most of the APrTEOS molecules.

Figure 4 shows ^{29}Si solid state n.m.r. spectra for the Nafion® precursor in which APrTEOS was sorbed and reacted under different conditions. The peaks in these spectra correspond very well to the T_n reference peaks that were established in *Figure 3* for APrTEOS that was simply reacted with itself. All samples were subjected to treatments that either interfere with or promote APrTEOS crosslinking.

All the samples in *Figure 4* were immersed in

APrTEOS for 4.5 days, but the other preparative conditions were different. The indicated weight uptakes, 13.9–16.6%, are considerable and reasonably close to each other. The lower spectrum corresponds to a second soaking in ethanol for 30 days—as opposed to the other much shorter 24-h second-soaks—with vacuum drying, but without heating, to intentionally produce a partially-reacted hybrid. To be sure, the spectrum for this hybrid does not depict a high degree of Si atom substitution about $CSiO_3$ groups. The middle spectrum corresponds to a sample that was intentionally incompletely dried of Flutec® prior to immersion in APrTEOS. An additional 3 h of evacuation of a different but equivalent Flutec®-imbibed sample that showed similar low weight loss when vacuum-dried for the same time, showed further Flutec® loss. This residual Flutec® may have affected APrTEOS crosslinking, perhaps through diffusional considerations, owing to plasticization. Thus, the combination of longer reaction time, higher temperature, and residual Flutec® conspires to give a higher degree of crosslinking than that for the sample represented by the bottom spectrum.

Formic acid treatment and curing at a higher temperature was employed to achieve a high degree of *in situ* APrTEOS reaction. Formic acid was shown by Sharp[21] to expedite gelation in TEOS systems. First, an as-received sample was soaked in Flutec® for 2 days at room temperature, after which it was removed and vacuum-dried at 102°C for 27 h. Then, the sample was immersed in APrTEOS for 4.5 days after which it was soaked in EtOH for two consecutive 24-h time periods to leach out excess APrTEOS. Finally, the sample was placed in formic acid for 69 h and then vacuum-dried at 120°C for 21 h. It is seen in the spectrum for this sample (*Figure 4*, top) that a rather high degree of condensation of SiOEt groups has in fact been achieved.

Figure 4 shows that for approximately the same uptake, manipulation of the curing temperature and time for each step, as well as addition of a sol–gel catalyst, can alter the nature of *in situ* APrTEOS crosslinking.

Contrasted with the i.r. analysis, these ^{29}Si n.m.r. results do not provide information relating to the degree of formation of sulfonamide linkages.

Mechanical tensile tests

Figure 5 consists of stress–strain profiles for Nafion® precursor films immersed in APrTEOS for different times; the plots are labelled according to the corresponding dry percent weight uptake. One of curves corresponds to an uptake that is higher than the asymptotic value of 18.3%. In the preparation of this sample there was a delay of 5 min between the time the sample was removed from the APrTEOS bath and the time at which it began soaking in EtOH for the purpose of leaching out unreacted APrTEOS. This additional time, during which the film was exposed to a 50% r.h. atmosphere, afforded APrTEOS molecules more opportunities to undergo reactions, which accounts for the inordinately-high uptake. These curves are somewhat similar to those seen for Nafion® sulfonate membranes in which silicon oxide phases were produced via *in situ* sol–gel reactions for TEOS[1,22]. Modulus and strength increase, and elongation-to-break decreases monotonically with increasing filler content. There is a difference, however, between these earlier nanocomposites[1,22] and

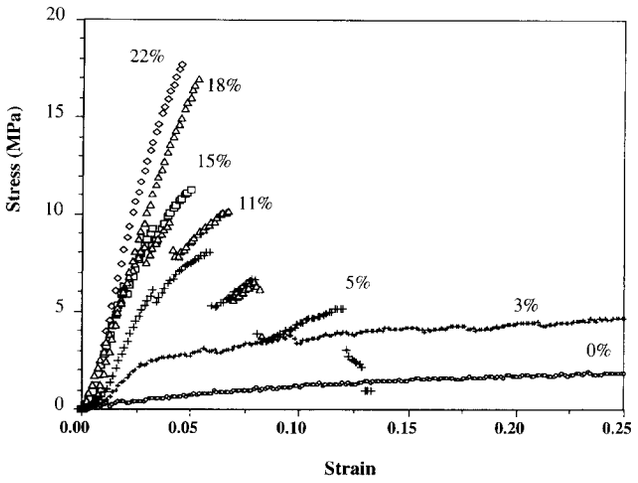

Figure 5 Stress vs strain for as-received Nafion® precursor and APrTEOS-treated precursors of indicated compositions

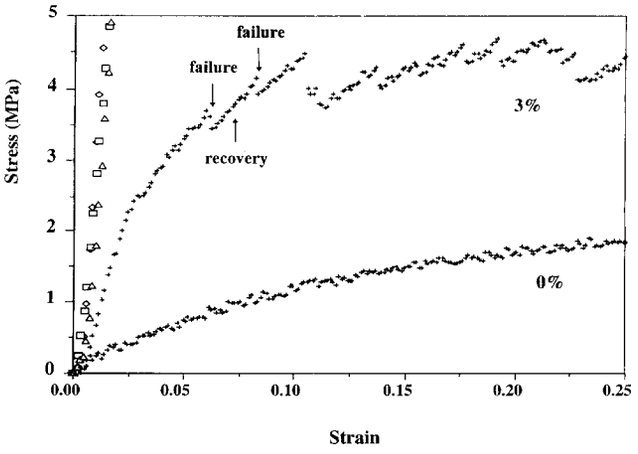

Figure 6 Expansion of vertical scale of stress–strain curves for the as-received Nafion® precursor and 3 wt% composite in *Figure 5* to illustrate the difference between instrumental noise and consecutive discontinuities in material response. A single failure → recovery → failure cycle is indicated for the 3 wt% composite by arrows

those particular hybrids in the present study that have less than 18% uptake due to *in situ* APrTEOS reactions. The difference is that the latter materials crack but subsequently recover under load as shown by intermittent, abrupt decreases in stress followed by slower increases in counteractive stress. These stepwise events are more apparent on closer inspection of the curves for the as-received and 3% uptake samples in *Figure 6*.

We point out that the noise seen along the curve in *Figure 6* for the as-received sample is associated with a statistical fluctuation in instrumental signal voltage

▶

Figure 7 Optical micrographs: (A) reticulated-mosaic surface morphology of 11 wt% composite (black bar, lower-left = surface crack; focus variation due to mild film warp); (B) smooth, featureless surface of as-received, untreated precursor (light region); (C) cumulative crack damage occurring away from ultimate fracture side for 3 wt% composite; double arrow indicating stress direction, is perpendicular to major cracks; cracks on opposite side appear as blurred dark lines parallel to major cracks on forward side; (D) fibrillar out-pulling from ultimate fracture edge of soft middle region for 3% composite. Striations, presumably of fibrillar origin, are seen near the edge. This fracture occurs when cracks on both sides coincide

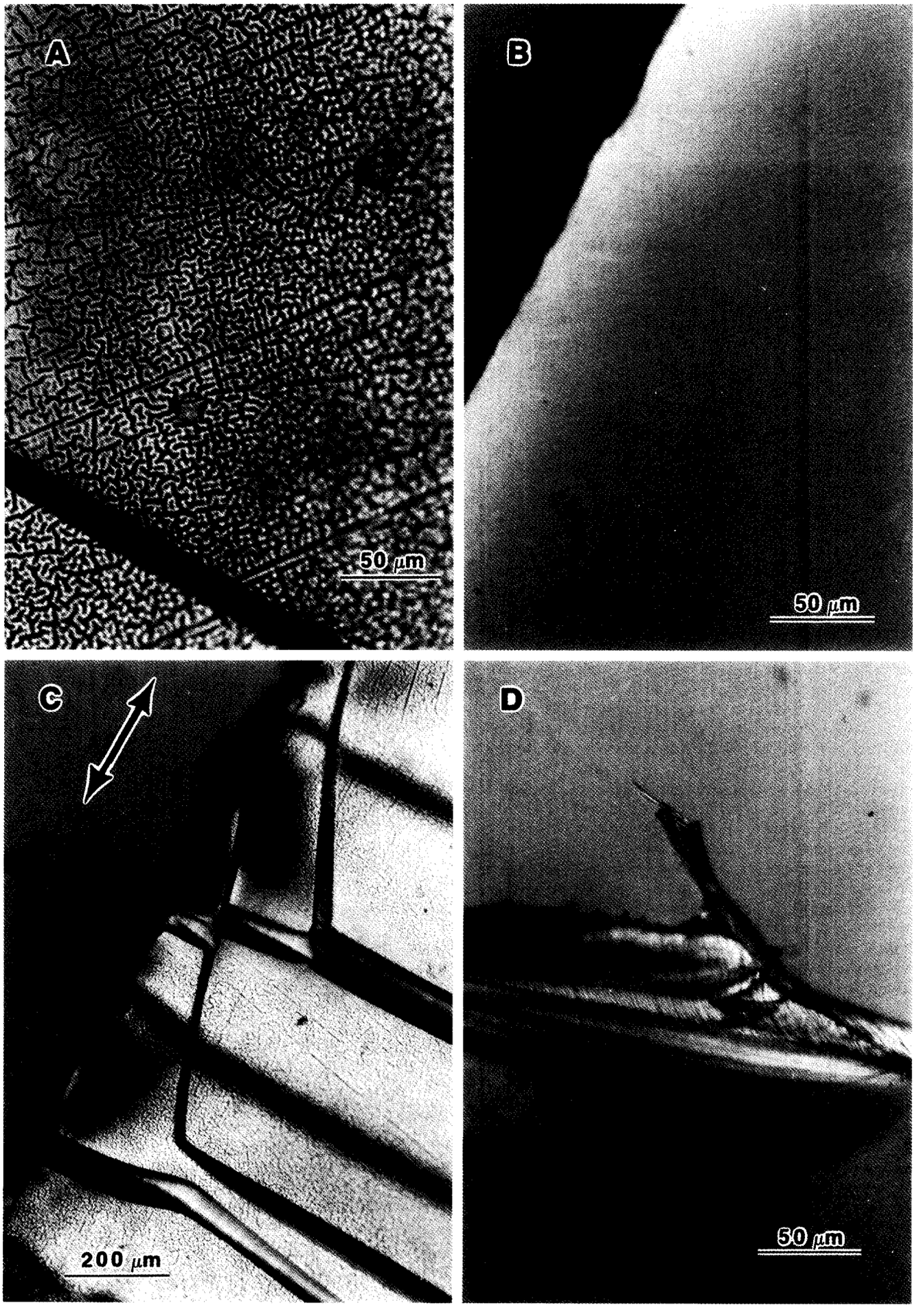
A
50 μm
B
50 μm
C
200 μm
D
50 μm

rather than with the actual mechanical response of the material. While this noise is also present on the 3% hybrid curve, the latter shows an organized series of deviations outside the range of random fluctuation. These stepwise drops along the 3% curve are interpreted in terms of a series of cracking events with partial stress recovery as discussed in the next section.

The curves for the 18% and 22% hybrids do not show this intermittent semi-failure. It is significant that the weight percents of these samples are either around or above the asymptotic value of 18.3% seen in *Figure 1*.

Morphology and silicon oxide concentration profile

Surface morphology. *Figures 7A* and *7B* are optical micrographs of an 11% hybrid and an as-received polymer, respectively. On comparing the surfaces at this magnification, it is seen that APrTEOS treatment changes the surface morphology from being smooth to having a distinct vermiculated pattern. This mosaic surface in *A* is unlike the cracked, smooth silica layers that often precipitate on the surfaces of Nafion®-H membranes during their immersion in TEOS/H_2O/alcohol solutions[3,23]. The three-dimensional nature of the heterogeneous surface in *A* is unknown.

The optical micrographs in *Figures 7C* and *7D* depict the manner in which the samples fail during elongation. The major cracks seen in *Figure 7C* are perpendicular to the draw direction (indicated by the double arrow) on either side of the sample. The zig-zag nature of the stress–strain curve for the 3% hybrid, which is more profound for hybrids having higher APrTEOS contents—but less than for 18%—is evidently due to a series of cracking steps within the APrTEOS-crosslinked, higher modulus outer layers on one or the other side. The onset of a given crack is not catastrophic as this damage is partially compensated for by having the unreacted polymer in the middle of the film assume a large portion of the load in the vicinity of the crack. While the unreacted regions of the polymer in the middle might be more mechanically compliant as suggested by the 0% curve, it is nonetheless noted that counteractive stresses can often recover to values greater than those existing before a given crack onset. Perhaps a recrystallization process in the semicrystalline tetrafluoroethylene regions, with drawing, can be implicated. Thereafter, a similar crack can initiate elsewhere on either side—but not both—and the process is repeated. After a series of such outer layer crack → inner layer stress recovery events, which produce the cumulative damage surface morphology seen in *Figure 7C* for 3%, two ultimate parallel cracks develop directly across from one another on opposite sides of the film. *Figure 7C* shows cumulative damage away from the fracture site and other pre-ultimate failure cracks on the opposite side are seen as blurry dark bars that are parallel to the major cracks on the forward side. In the ultimate failure scenario, elongation of the softer interior occurs with greater facility than for the condition where an unmatched crack occurs on a given side. Thus, when matched cracks develop opposite each other on both surfaces, the load is redistributed over a smaller cross-sectional area of the softest phase; failure occurs when the softer material breaks. *Figure 7D* shows pulled-out softer material at the edge of a crack. This type of failure is reminiscent of the 'cumulative weakening' model for failure in

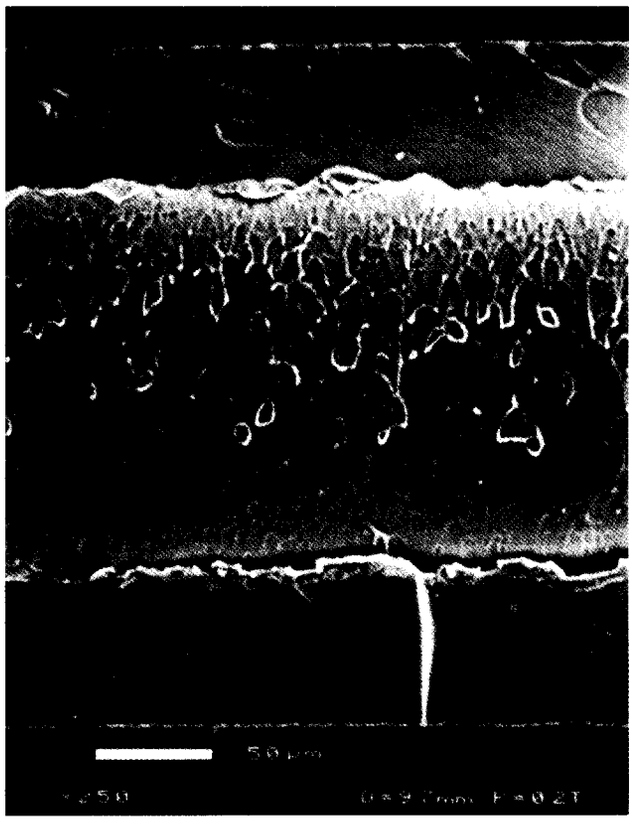

Figure 8 ESEM micrograph of fracture surface for 4.6% composite showing distinct highly crosslinked outer layers and the lightly crosslinked middle

cases where soft matrices surround higher modulus reinforcements[24,25]. In this model, the higher modulus reinforcement, typically a fibre, fails prior to the surrounding matrix.

Fracture morphology. A typical region of a freeze-fractured cross section observed by ESEM is seen in *Figure 8* for a 4.6% composite. There are no surface-attached layers, although the weight uptake for this sample is low. There are sharply-defined material fronts located inward from both surfaces of the film. Covitch *et al.*[7] observed similar 'reaction' fronts in his experiments with ethylenediamine-treated Nafion® sulfonyl fluoride films and discovered that the reaction is essentially complete within these two outer zones. The results of our *FT* i.r./ATR studies, which apply to the outer layers but not to the middle region, indicate rather complete reactions, as well. We observe that the middle region has the fracture morphology of the unreacted precursor and the outer regions that of a totally-reacted sample. The outer regions resemble the fracture surfaces of cross-linked epoxy materials[26] while the interior of this 4.6% hybrid shows a more unique dimpled/torn surface. The interface between the two regions may have separated in places while remaining intact elsewhere. This may, however, be a result of the manner of fracture. Since the stiff wavelike film was bent in order to facilitate a break, one side may have experienced compression-type failure while the other experienced tensile failure.

Inorganic composition profile. Although there appears to be a distinct reaction front from the morphological perspective, some APrTEOS molecules might

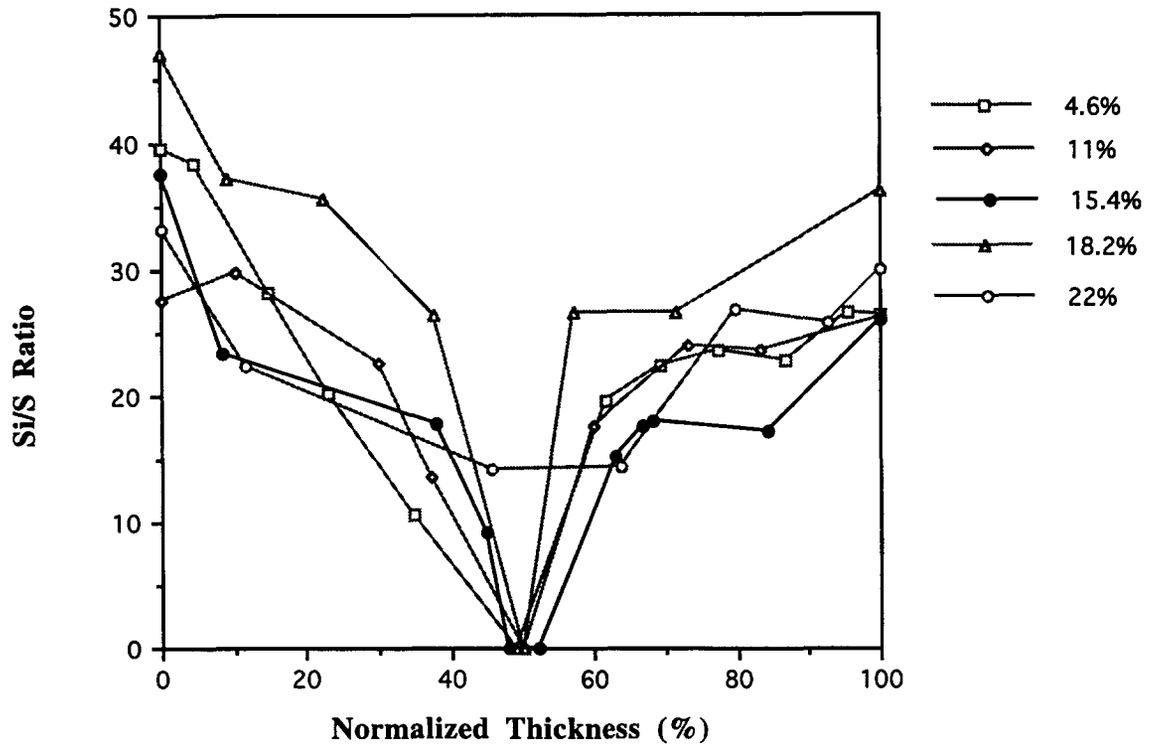

Figure 9 Typical Si/S EDAX elemental intensity ratio vs probe position profiles on fracture surfaces across membrane thickness direction for wt% uptakes indicated at right of figure. All samples are normalized in that the horizontal axis refers to percent of total thickness from left surfaces

have diffused and reacted beyond this visual plane. Covitch *et al.*[7] discuss an incompletely-reacted frontal zone that is quite relevant in our interpretation. *Figure 9* shows typical Si/S EDAX elemental intensity ratio profiles across the membrane thickness for a number of indicated weight uptakes.

None of the concentration profiles appear as mirror-image step functions on either side of the mid-plane of the films as suggested by *Figure 8*. There are no sharp Si composition boundaries from the EDAX perspective. The sharp visual boundaries may be due to a division of the material into zones having drastically different properties related to mechanical failure rather than to strict segregation of reacted APrTEOS. Only the highest-filled polymer (22%) has detectable Si in the middle.

It is interesting that while the 18.2% sample essentially incorporates the asymptotic quantity of reacted APr-TEOS molecules seen in *Figure 1*, progressively fewer SO_2F groups would seem to be reacted in proceeding toward the middle according to the corresponding EDAX profile. These unreacted SO_2F groups would, however, be undetected by the *FT* i.r./ATR method which only probes near-surface regions.

It is possible that the Si distributions for different samples may not be quantitatively comparable in a strict sense because of slight variations of fracture surface orientation in the ESEM. For a given constant stage tilt, the fracture surfaces on samples may not be exactly normal to the beam and for different samples may be oriented at somewhat different angles relative to the detector. The apparent asymmetry of Si/S ratio profiles might be explained in terms of this local orientation variation and different associated probe depths. Further, for the side at '0' distance on the horizontal axis in *Figure 9*, we mention that the probe did not penetrate the sample through the adjacent side because the tilt of the sample 'buries' the probe. On the other side, the probe may have penetrated the sample when the probe is placed at the tilted edge. While *Figure 9* should be interpreted on a semiquantitative level, these EDAX experiments nonetheless demonstrate that there are no sharp Si gradients across the membrane thickness direction.

Thermal analysis

Thermogravimetric analysis. T.g.a. scans were obtained to understand the degradation of a highly-filled composite so as to assist in the interpretation of the d.s.c. results. *Figure 10* shows traces for a 19% composite cured at 102°C for 24 h, and for independently-reacted (pure) APrTEOS that was likewise cured at 102°C. The pure APrTEOS-derived sample gradually loses weight up to 280°C prior to experiencing a sharp weight loss. The gradual loss up to 280°C is most likely due to the release of volatiles that are generated by condensation reactions while the sharp loss is clearly chemical degradation. In contrast, the composite, after essentially no weight loss, abruptly loses about 10% of its weight at 270°C, followed by a catastrophic loss around 280°C. Pending an off-gas analysis, it is assumed that the weight loss of the composite is largely associated with breaking C–C bonds in the sidechain-attached-HNPrSi(O–)$_3$ groups since these loss temperatures are below the thermal decomposition temperature of Nafion® itself.

The melting point of the Nafion® precursor is in a range around ~265°C, although exact T_m depends on equivalent weight[10]. However, Gierke *et al.*[10] observed wide angle X-ray diffraction patterns up to 275°C for this polymer. It appears then, for the composite in *Figure 10*, that decomposition proceeds just after semicrystalline order disappears. This fact would be consistent with the difference in t.g.a. traces in *Figure 10* in that both materials suffer catastrophic decomposition at around 275°C, but significant weight loss is retarded in the

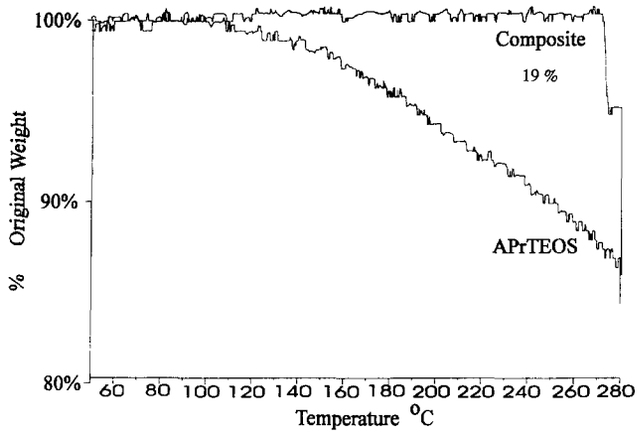

Figure 10 T.g.a. plots for sol–gel-reacted APrTEOS (not *in situ*), cured at 102°C, and 102°C cured, 19% composite

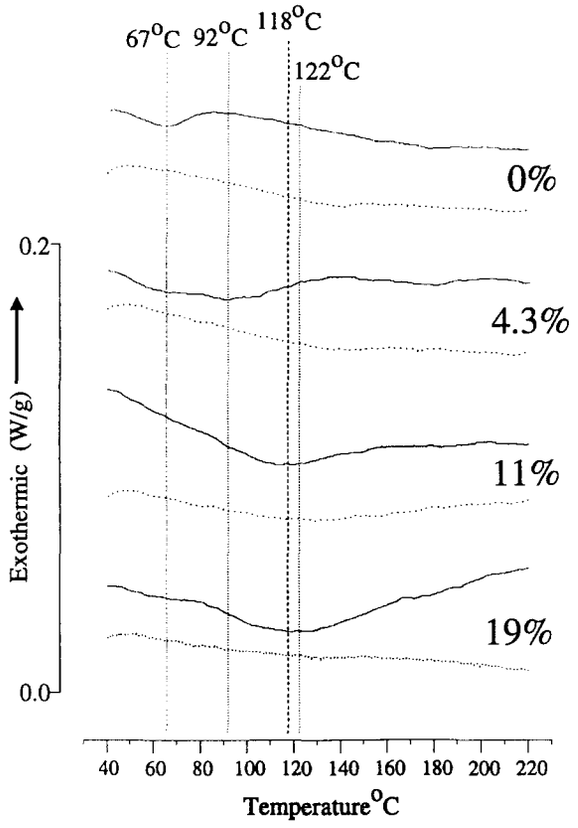

Figure 11 1st (solid) and 2nd (dotted) d.s.c. heating curves for as-received (0%) precursor and indicated composites noting transition peak positions

composite until this temperature is reached. It is important that future studies address the dependence of T_m on filler content for the composites.

Differential scanning calorimetry. Given the onset temperature of primary decomposition as established by the above t.g.a. studies for a rather highly filled membrane, the temperature range for d.s.c. investigation relevant to these studies was chosen as being from ambient to 230°C. This range, of course, precludes investigation of the effect of crosslinking on the melting as well as subambient transitions. *Figure 11* shows first and second heating curves for the as-received polymer and for the 4.3, 11, and 19% composites on a rather

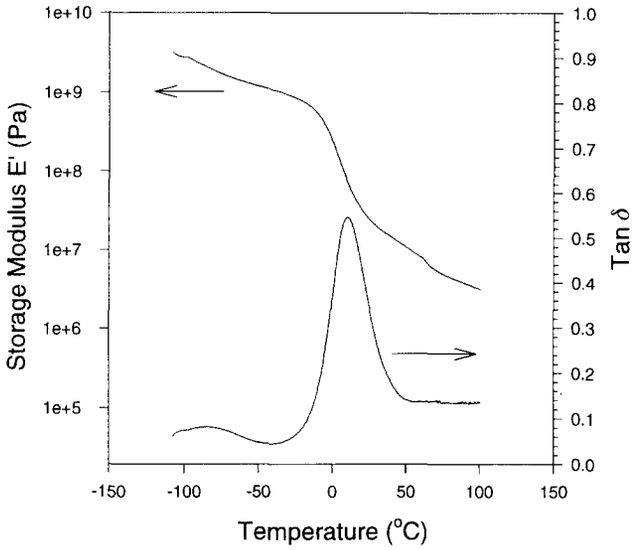

Figure 12 Dynamic mechanical storage modulus (E') and loss tangent ($\tan\delta$) vs temperature (tensile mode deformation at 1 Hz) for the precursor form

expanded vertical scale. The first cooling curves, which are identical to the second cooling curves for each composition, show no significant thermal activity.

Each scan shows a broad, weak endothermic peak that monotonically shifts to higher temperatures with increasing filler content during the initial heating cycle. While this feature might be considered to result from volatile release owing to imbibed solvent or thermally-driven condensation reactions of SiOR groups, these samples were dried prior to the d.s.c. experiment. Furthermore, this peak appears for the untreated film as well as for the composites. Importantly, no significant weight loss was seen in this temperature range by t.g.a. even for the 19% composite. Therefore, we conclude that this is a physical order–disorder transition in the fluoropolymer. The disappearance of this transition during the second run is, in general terms, viewed as being due to disorder that was frozen-in during the quenching from 230°C. At present, the exact nature of this d.s.c. transition, in terms of specific molecular mechanisms, is not clearly understood, but it clearly occurs at too low a temperature to be considered a melting event.

Figure 12 shows the dynamic mechanical behaviour of the precursor in the temperature range of −100 to 125°C. The drop in storage modulus, E', and the maximum in the loss tangent, $\tan\delta$, clearly indicate an event resembling a glass transition centered at *ca* 10°C. By correlating these data with the data in *Figure 11*, it appears that the order–disorder transition in the d.s.c. experiment occurs once long range chain segmental mobility is thermally activated. It is seen in *Figure 12* that the $\tan\delta$ peak has essentially subsided by the time the temperature of 50°C is reached. Moreover, as chain segmental mobility becomes increasingly more restricted with increasing degree of the APrTEOS reaction which creates crosslinks, glass transition temperature (T_g), and consequently the temperature of the order–disorder transition, monotonically increase. The fact that the d.m.a. transition occurs just before the d.s.c. transition would seem to be more than fortuitous. Perhaps the difference in the temperature ranges over

which these transitions occur is due to the fact that the time scales for the thermal (d.s.c.) and mechanical (d.m.a.) experiments are different. It is well-known that increasing the rate of heating in a d.s.c. or d.m.a. experiment, or increasing the oscillation frequency in a d.m.a. experiment, will cause an increase in observed T_g.

The broadness of this order–disorder transition observed by d.s.c. is attributed to the following form of microstructural heterogeneity. Consider a straight line that extends from the surface of a reacted film to the centre. With reference to *Figure 9*, the degree of crosslinking, assumed to be proportional to the Si concentration at a given point, should decrease in this direction along the line. Therefore, as the degree of chain segmental mobility increases in this direction, T_g varies in decreasing fashion. While the transition monitored by d.s.c. is manifest as a bulk property, the broad distribution of microscopic thermal events due to considerable differences in local chemical environments, is reflected in the breadth of the transition.

CONCLUSIONS

The goal of this work was to generate perfluoro-organic/inorganic hybrid materials by utilizing the melt-processible sulfonyl fluoride precursor of Nafion® membranes as a sol–gel reaction medium for APrTEOS. Gravimetric studies showed in a general way that the diffusion-mediated reaction of APrTEOS with SO_2F groups can be controlled and that a high degree of reaction is possible. *FT*i.r./ATR studies of near-surface regions support these results and show that sulfonamide linkages are formed and condensation reactions of SiOR groups provide covalent crosslinking of chains. I.r. as well as gravimetric evidence suggests that there is a soluble fraction of the polymer that is extracted upon soaking in the solvent Flutec®. ^{29}Si solid state n.m.r. spectra of pure APrTEOS sol–gel-derived samples showed discrete peaks that reflect the distribution of x in $CSi(OR)_{4-x}(OSi)_x$ groups, and hence the degree of crosslinking. With regard to the composites, formic acid treatment plus high temperature plus long time resulted in a high degree of polymer crosslinking through this form of sidechain coupling. Mechanical modulus and strength increase while elongation-to-break decreases with increasing filler content. Hybrids with <18% uptake accumulate cracks within the crosslinked outer layers, each signalled by a drop in stress followed by stress recovery. The onset of these pre-failure cracks is not catastrophic as the unreacted polymer in the middle of the film assumes a major portion of the load in the crack vicinity. While ESEM showed that there are sharp visual material fronts located inward from both surfaces, EDAX suggested that there are no sharp Si composition boundaries as [Si] can extend beyond material fronts toward the middle of films. D.s.c. experiments revealed a broad, weak endothermic event on first heating that peaks at 67°C for the precursor and shifts to higher temperatures, while broadening, with increasing filler content. For the unreacted precursor, this d.s.c. transition occurs at a temperature just above a T_g detected by dynamic mechanical means. In general terms, this upward temperature shift indicates progressively-restrictive molecular motions owing to greater crosslinking while peak broadening reflects an increasingly nonhomogeneous environment in which this relaxation takes place. This view is consistent with the distribution of morphology and Si composition variation observed via ESEM/EDAX.

The interesting conversion of the smooth, featureless membrane surface morphology to a vermiculated pattern via APrTEOS treatment might yield a functional substrate template on which catalytic metals, metal oxides or semiconductors might be deposited.

In future studies, gas permeability experiments will be conducted over a spectrum of diffusants of various molecular sizes and polarities with the view that permeation vs applied pressure plots will yield information relating to diffusant-hybrid interactions and multiphase morphological features. These robust hybrid materials might possess useful gas permselectivity properties.

ACKNOWLEDGEMENTS

This material is based partly upon work supported by a grant from the National Science Foundation/Electric Power Research Institute (Advanced Polymeric Materials: DMR-9211963). This work was also sponsored in part by the Air Force Office of Scientific Research, Air Force Systems Command, USAF, under grant number AFOSR F49620-93-1-0189. The US Government is authorized to reproduce and distribute reprints for Governmental purposes notwithstanding any copyright notation thereon. The donation of Nafion® membranes by the E. I. du Pont de Nemours & Co., through the efforts of J. T. Keating, is appreciated. We acknowledge M. A. F. Robertson, Department of Polymer Science, University of Southern Mississippi, for assistance in the interpretation of spectra.

REFERENCES

1 Mauritz, K. A., Storey, R. F. and Jones, C. K. in 'Multiphase Polymer Materials: Blends, Ionomers and Interpenetrating Networks', ACS Symp. Ser. 395 (Eds L. A. Utracki and R. A. Weiss), Amer. Chem. Soc., Washington DC, 1989, p. 401
2 Mauritz, K. A. and Warren, R. M. *Macromolecules* 1989, **22,** 1730
3 Mauritz, K. A., Stefanithis, I. D., Davis, S. V., Scheetz, R. W., Pope, R. K., Wilkes, G. L. and Huang, H.-H. *J. Appl. Polym. Sci.* 1995, **55,** 181
4 Deng, Q., Mauritz, K. A. and Moore, R. B. in 'Hybrid Organic-Inorganic Composites', ACS Symp. Ser. 585 (Eds J. E. Mark, P. A. Bianconi, and C. Y.-C. Lee), Amer. Chem. Soc., Washington DC, Ch. 7, 1995
5 Deng, Q., Moore, R. B. and Mauritz, K. A. *Chem. Mater.* 1995, **7,** 2259
6 Shao, P. L., Mauritz, K. A. and Moore, R. B. *Chem. Mater.* 1995, **7,** 192
7 Covitch, M. J., Lowry, S. R., Gray, C. L. and Blackford, B. in 'Polymeric Separation Media' (Ed A. R. Cooper), Plenum Pub. Corp., New York, 1982, p. 257
8 Hsu, W. Y. *Macromolecules* 1983, **16,** 745
9 Grot, W. G. *U.S. Patent* 3 969 285 July 13, 1976
10 Gierke, T. D., Munn, G. E. and Wilson, F. C. *J. Polym. Sci. Polym. Phys. Edn* 1981, **19,** 1687
11 Cory, D. G. and Ritchey, W. M. *J. Magn. Reson.* 1988, **80,** 128
12 Ostrowska, J. and Narebska, A. *Colloid Polym. Sci.* 1983, **261,** 93
13 Liang, C. Y. and Krimm, S. *J. Chem. Phys.* 1956, **25,** 563.
14 Weast, R. C., Astle, M. J. and Beyer, W. H. (Eds) 'CRC Handbook of Chemistry and Physics', 67th Edn, CRC Press, Boca Raton, 1987, F-199

15 Conley, R. T. 'Infrared Spectroscopy', 2nd Edn, Allyn and Bacon, Inc. Boston, 1975, p. 198.
16 'CRC Handbook of Chemistry and Physics' (Eds R. C. Weast, M. J. Astle and W. H. Beyer), 67th Edn, CRC Press, Boca Raton, 1987, p. 147
17 Hsu, W. Y. *Macromolecules* 1983, **16,** 745
18 Falk, M. in 'Perfluorinated Ionomer Membranes', ACS Symp. Ser. 180 (Eds A Eisenberg and H. L. Yeager), Amer. Chem. Soc., Washington DC, 1982, Ch. 8
19 Diehl, P., Fluck, E. and Kosfeld, R. (Eds) 'Oxygen-17 and Silicon-29 NMR, Basic Principles and Progress', Vol. 17, Springer-Verlag, New York, 1981, p. 184
20 Spindler, R. and Shriver, D. F. *Macromolecules* 1988, **21,** 648
21 Sharp, K. G. *J. Sol–Gel Sci. Technol.* 1994, **2,** 35
22 Davis, S. V. and Mauritz, K. A. *Am. Chem. Soc. Polym. Prepr.* 1992, **33**, 363
23 Davis, S. V. *PhD Thesis*, University of Sothern Mississippi, Hattiesburg, Mississippi, 1995
24 Rosen, B. W. 'Fiber Composite Materials', Am. Soc. Metals, Metals Park, 1965, Ch. 3
25 Hull, D. 'An Introduction to Composite Materials', Cambridge University Press, New York, 1981, p. 133
26 Purslow, D. *Composites* 1986, **17**, 289